Large Area Hybrid Photodiodes

C. Joram[a]

[a]CERN, EP Division, CH-1211 Geneva 23, Switzerland

Hybrid Photodiodes (HPD) represent one of the most promising options for high granularity single photon detection. HPD's are photodetectors consisting of a photocathode, which is deposited on the inner side of the entrance window, and a solid state sensor encapsulated in a vacuum envelope. HPD's combine the high sensitivity of photomultiplier tubes with the excellent space and energy resolution of solid state detectors.

After reviewing the physical principles of HPD's the article gives a short overview of the history of this detector. A number of commercially available devices will be discussed. Current and future applications in high energy physics lie in the fields of scintillator readout (calorimetry, fibre tracking) and Cherenkov light detection. It is for the latter application that various large area Hybrid Photodiodes are currently under development.

1. Physical principles of Hybrid Photodiodes

Similar to conventional photomultiplier tubes (PMT) Hybrid Photodiodes consist of a vacuum envelope with a transparent front window (see Fig 1). A photocathode which is deposited on the inner side of the window converts light quanta into electrons. These photoelectrons are emitted from the photocathode and accelerated by a potential difference ΔV of the order of 10 to 20 kV directly onto the silicon sensor which is usually kept at ground potential. The electric field can be shaped by means of electrodes in order to obtain certain electron-optical properties, e.g. a linear demagnification between the photocathode and the silicon sensor. The absorbed kinetic energy of the photoelectron gives rise to the creation of electron-hole pairs, which in the depleted silicon sensor results in a detectable current.

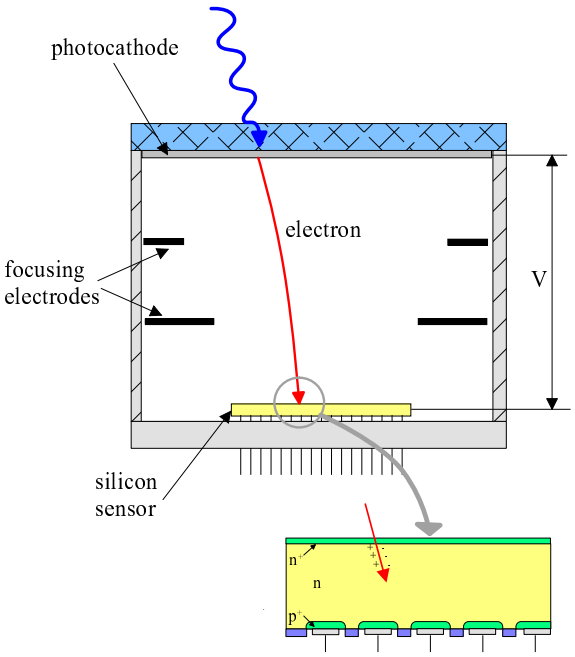

Figure 1. Main components and principle of operation of a HPD.

1.1. Windows and photocathodes

Depending on the specific application HPD's can be produced with various photocathode and window types. The key parameters are the energy threshold of the photocathode, its spectral sensitivity $S(\lambda)$ or quantum efficiency $\varepsilon_Q(\lambda)$ and the cut-off wavelength of the window. Widely used photocathodes are of the bialkali (K_2CsSb) or multialkali (SbNaKCs) type. For special applications also VUV sensitive CsTe or negative electron affinity cathodes (GaAs, GaAsP, InGaAsP) are available. The latter are characterised by high sensitivities in the red and infrared part of the optical spectrum and are fabricated by molecular beam epitaxial growth. The effective sensitivity of the HPD is of course limited by the transmission of the entrance window, with cut-off wavelengths ranging from 300 nm for lime glass down to 160 nm for

fused silica quartz and even 105 nm for LiF single crystal windows.

1.2. Silicon sensor and gain mechanism

The main difference compared to photomultiplier tubes lies in the mechanism by which the detector gain is achieved. In an HPD the accelerated photoelectrons bombard the silicon sensor and penetrate it to a depth of a few μm. The number of created electron-hole pairs per photoelectron, i.e. the gain of the device, is given by

$$G = (\Delta V - E_0)/W_{e-h} \quad (1)$$

with $W_{e-h} = 3.6eV$ being the average energy needed for the creation of a single electron-hole pair in silicon. E_0 describes the energy ($\approx$ 1-2 keV) which is lost in non-active material layers of the Silicon detector (aluminium contact layer, n^+ layer). The design of the silicon sensor has therefore to be optimised for minimal dead layer thickness. For a potential difference ΔV = 20 kV a gain of about 5000 is achieved. The small penetration depth of the electrons results in sub-ns rise- and fall-times. The charge amplification process is purely dissipative and non-multiplicative, i.e. in contrast to a PMT, where large gain fluctuations are due to the Poisson distributed number of electrons after the first dynode, the variation of the HPD gain is given by

$$\sigma_G = \sqrt{GFm} \quad (2)$$

where $F \approx 0.1$ denotes the Fano factor for silicon and $m = 1, 2, 3...$ the number of photoelectrons. In practice these variations are much smaller than the noise of the readout electronics which will finally determine the energy resolution of the HPD.

When electrons with relatively low energies (20 keV) impinge on the silicon sensor, there is a probability $\alpha_{Si} \approx 0.2$ that the electron will be back-scattered into the vacuum, hence depositing only a fraction of its energy in the silicon. As shown in Figure 2 [1] this gives rise to a continuous background on the low energy side of each peak. This effect finally limits the photon counting performance of the detector when irradiated with a relatively large average number of photons.

The solid line in Fig. 2 is the result of a fit based on a simple model of the backscattering effect, which finally allows to describe the spectrum by only three

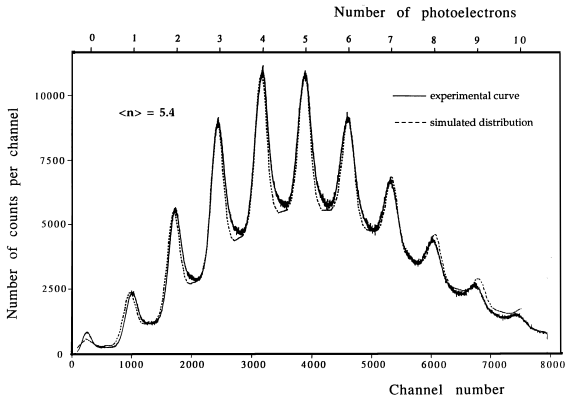

Figure 2. Pulse height spectrum obtained with a single pixel HPD (from ref. [1]).

parameters: m, α_{Si} and σ, where σ is the Gaussian width of the peaks, identical for all peaks. A more general analysis of photoelectron spectra using a "light spectra sum rule"[2] has recently been published.

Segmenting the silicon sensor in diode strips, pixels or pads which are read out individually results in a photodetector with high spatial resolution. The spatial resolution of the HPD is however not only determined by the granularity of the sensor but also by the electron optical properties of the HPD. Distortions of the electric field as well as the distribution of the emission angle and energy of the photoelectrons at the photocathode lead to a reduced resolution, characterised by the point spread function. Carefully designed optics are able to partly correct for the aberrations and achieve point spread functions below 50 μm. A natural limit of the achievable spatial resolution is imposed by the phenomenon of charge sharing between neighbouring readout pixels. Due to transverse diffusion along the drift through the bulk, the charge cloud at the pixel plane arrives as a Gaussian distribution with a width of the order of σ = 10 μm. In case of very small pixels (<50 μm) the total detectable charge will be shared by several pixels where the charge detected by the individual pixel may fall below the detection limit (because of noise in case of analogue readout or detection threshold for digital readout sys-

tems).

Above a certain number of channels (a few hundreds) it becomes impractical to readout the detector through individual vacuum feedthroughs. In this case the readout electronics has to be integrated in the vacuum envelope. The signals, either digital or analog, are then read out in a multiplexed scheme through a relatively small number of feedthroughs. This technique requires components which are conform with the tube processing (vacuum bake-out) and long term operation in vacuum (minimum outgasing and low power consumption).

1.3. HPD designs

Hybrid Photodiodes can be classified with respect to their electron optical design. There are basically three different designs, which are schematically shown in Figure 3:

- Proximity focusing
  This design leads to compact and, because of the small gap between photocathode and silicon sensor, highly B-field tolerant detectors. Because there is no demagnification, the photosensitive area of the detector is limited to the size of the silicon sensor.
- Cross focusing
  A cross focusing design is chosen when high resolution imaging is required because the electrostatic lens effect largely compensates for the spread of the photoelectron velocity and emission angle at the photocathode. Small pin cushion shape distortions at large distance from the optical axis are typical for this design. Cross focused tubes allow for strong demagnification, imply however a relatively large distance between cathode and solid state sensor, which results in a pronounced magnetic field sensitivity.
- Fountain focusing
  The fountain focusing design represents an alternative to the cross focused HPD if a reduced spatial resolution is acceptable. The optics does not correct for the emission angle distribution but results in a simple and compact tube design combined with a linear demagnification over the full acceptance. The sensitivity to magnetic fields is similar to the cross focusing design.

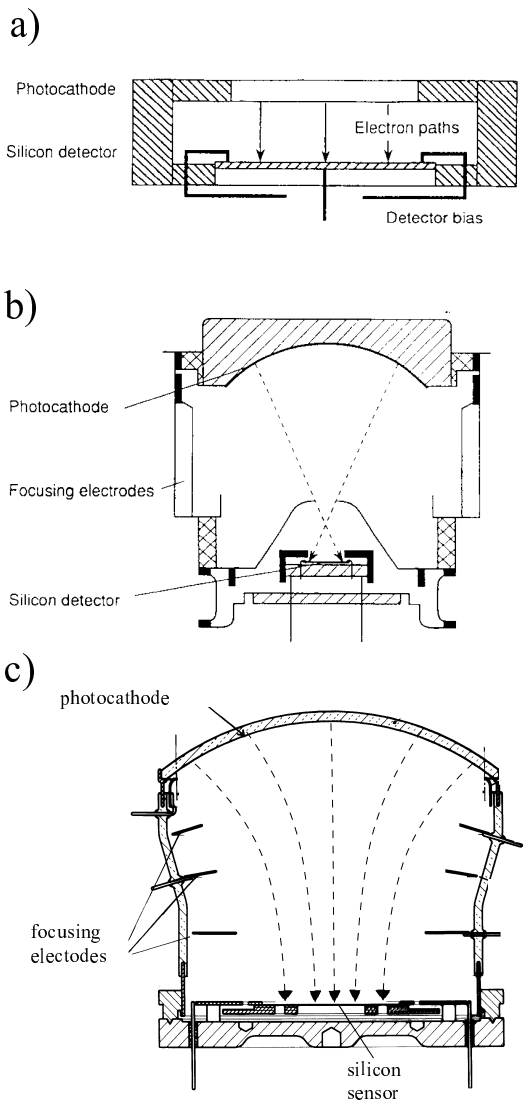

Figure 3. Designs of Hybrid Photodiodes: a) proximity focusing, b) cross focusing, c) fountain focusing.

1.4. Comparison with other photodetectors

The combination of high sensitivity cathode, non-multiplicative gain mechanism and segmented silicon sensor make the HPD a fast photodetector which offers very good spatial and energy resolution, as well as excellent photon counting capability. In Table 1 a

Table 1
Comparison of HPD's with various other photodetectors (MAPMT = Multi Anode PMT, APD = Avalanche Phododiode, CCD = Charge Coupled Device, VLPC = Visible Light Photon Counter).

type	ε_Q[%]	gain	photon counting	spatial resolution	speed	remarks
HPD	≈ 25	$\approx 10^3$	yes	high	high	1)
PMT	≈ 25	$\approx 10^6$	limited	no	high	1)
MAPMT	≈ 25	$\approx 10^6$	no	medium	high	1)
PIN diode	≈ 80	1	no	high	high	2)
APD	≈ 80	≈ 100	limited	no	high	2,3)
CCD	≈ 80	1	no	high	low	4,5)
VLPC	≈ 70	$\approx 10^6$	yes	no	high	6)

1) Spectral sensitivity depends on cathode type, $\varepsilon_Q \approx 25\%$ at 400 nm .
2) High quantum efficiency in red/infrared region, decreasing towards the UV.
3) Arrays of APD's are under development [3,4].
4) High ε_Q only when illuminated from backside.
5) Photon counting has recently been demonstrated with electron bombarded CCD's [5].
6) Operation requires cooling to LHe temperatures [6].

rough comparison is made between HPD's and various other photodetectors concerning their quantum efficiency, the achievable gain, spatial resolution and speed.

2. Overview of HPD history

The attractiveness of using a solid state diode as electron multiplication element and its superiority to dynode-based cascade multiplication was recognised already around 1960 [7,8]. The first phototubes with individual reversed biased silicon sensors, i.e. HPD's, have been demonstrated to work around 1965 [9–11].

In 1971 Beaver and McIlwan [12] realized a HPD with a silicon substrate segmented into a linear array of 38 individual diodes (0.101 mm pitch) which they called *Digital Multichannel Photometer* and for which they obtained an US patent. The device (see Figure 4), built for applications in astronomy, adopted the proximity focusing principle and comprised a solenoid magnetic field which allowed for scanning of a 2D optical image. The photoelectrons could be accelerated to typically 30 keV.

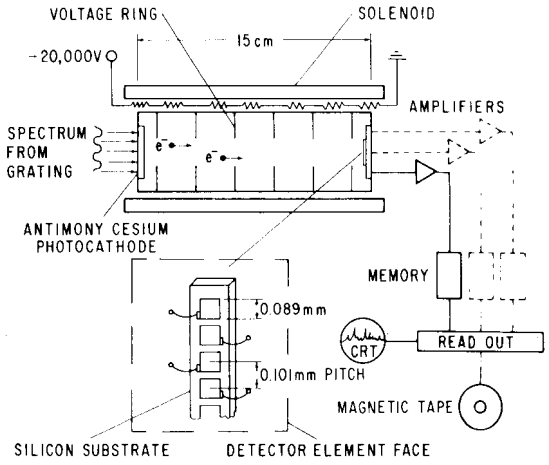

Figure 4. Schematic drawing of the Digital Multichannel Photometer realized in 1971 [12]. It is equipped with a linear silicon array of 38 diodes.

A further step in the HPD history is marked by the development of the so-called DIGICON tubes around 1980 [13]. The tube which from its basic design resembles the 38 pixel tube discussed above, comprises a linear diode array of 512 elements ($40 \times 500\ \mu m^2$, 50 μm pitch), proximity focusing (22 kV cathode voltage) and a magnetic solenoid field. The Faint Object Spectrograph, which is part of the Hubble Space Telescope (HST), has been equipped with two DIGICON tubes, one with a blue-peaked bialkali and one with a red sensitive multialkali S20 photocathode. Since the launch of the HST in 1990 the DIGICON

tubes have significantly contributed to the discovery and characterisation of extremely distant astronomical objects.

For a long time the developments described above did not receive any attention by the high energy physics community. In 1987 De Salvo [14,15] practically re-invented the HPD principle when looking for fast photodetectors which can be operated in strong magnetic fields. The specific application which he had in mind was scintillator readout of a calorimeter of the SSC detector.

A further important milestone is marked by the development of the ISPA (Imaging Silicon Pixel Array) tube[16] in 1994. The detector, built in the framework of CERN's RD7 and RD19 programs for the readout of scintillating fibres (fibre tracker), incorporated for the first time the readout electronics inside the vacuum tube. This allowed the use of a finely segmented pixel array sensor ($64 \times 16 = 1024$ pixels of 75×500 μm^2) which was bump bonded to a binary readout chip which had the same geometry as the sensor. The readout in parallel line mode resulted in total readout times of the order of 10 μs. Figure 5 [17] shows an image of a lead mask obtained with the ISPA tube. It demonstrates the spatial resolution capabilities of the HPD technique. Scintillation light of a YAP crystal was observed through holes of 0.6 mm diameter. The distance between the holes was 1.2 mm and 2.4 mm, respectively.

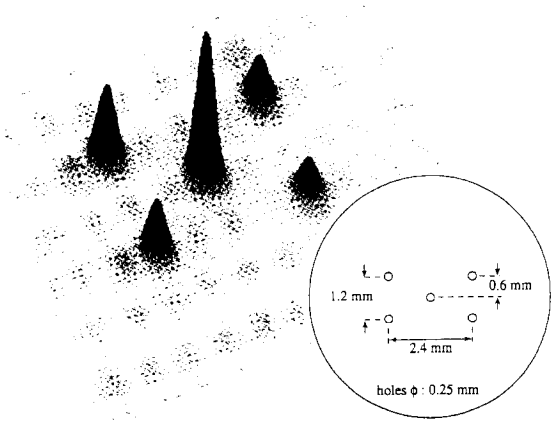

Figure 5. An image of a lead mask obtained with the ISPA tube [17].

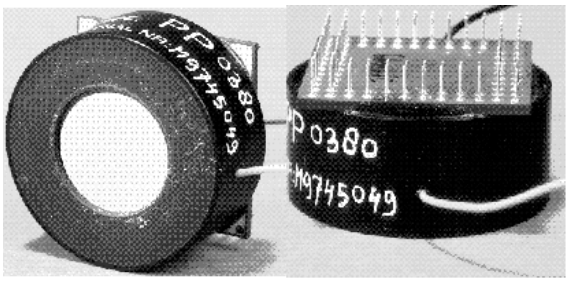

Figure 6. Photograph of a proximity focused multipixel HPD fabricated by DEP.

3. Commercially available HPD's

For the time being only a few suppliers fabricate HPD's, and so far only one company produces *off the shelf* HPD's with segmented silicon sensors.

3.1. DEP

The Dutch company DEP (Delft Electronic Products) provides a series of single and multipixel HPD's. Electrostatically focused single pixel devices are available with a sensitive diameter of up to 40 mm. Proximity focused multipixel devices (see Fig. 6) with up to 61 pixels are produced with active diameters of up to 25 mm. Various photocathode types (solar blind, bialkali, multialkali) can be chosen. A drawback of the currently available detectors is their modest active area fraction (well below 50%) which represents a serious obstacle for certain applications. As will be discussed in the section 4, DEP is currently involved in various projects aiming at the development of large area HPD's.

3.2. Hamamatsu

Hamamatsu (Japan) fabricates a proximity focused HPD with 8 mm sensitive diameter which is equipped either with a Si PIN diode or an avalanche diode. In the latter case the gain of the detector can be as high as 65,000, however at the expense of the energy resolution. For large area application a multipixel arrangement is in preparation [18], where a matrix of HPD's

are assembled in a single potting case. The active area fraction does however not exceed 20%.

3.3. INTEVAC

The American supplier INTEVAC has developed an electrostatically focused single pixel HPD which is equipped with a GaAs or GaAsP photocathode. The achievable quantum efficiency (45% at λ = 500 nm) is significantly superior to alkali antimonide cathodes, particularly in the red and infrared part. In collaboration with a group from Max-Planck-Institute Munich [19,20] the detector is currently being optimised in view of a possible application in an Air Cherenkov telescope.

4. Development of large area HPD's

4.1. Potential applications of HPD's in high energy physics

Hybrid Photodiodes are attractive candidates for many photodetection applications. We restrict our discussion to applications in high energy physics, although a significant potential exists for applications in other fields like medical imaging [21] and astrophysics (Air Cherenkov telescopes).

In high energy physics current and future potential applications of HPD's lie mainly in the three following areas:

- Calorimetry
  The readout of scintillators can profit from the robustness of proximity focused HPD's in strong magnetic fields, their intrinsicly high speed and dynamic range of 8 decades in charge [22]. If the scintillators are read out via fibres, the segmentation of the HPD reduces the number of tubes and hence may lead to significant cost reductions. The CMS collaboration has recently decided to equip a large part of the hadron calorimeter with commercial proximity focused multipixel HPD's from DEP [23]. The HPD's will be operated in an axial B-field of 4 T.

- Time Of Flight and Fibre Tracking
  As mentioned above the ISPA tube was originally developed for fibre tracking purposes. It is again the segmentation (cost reduction), the high speed (use of track information in 1^{st} level trigger) and the possible operation in magnetic fields which are the most attractive features of a HPD. In the experiment FINUDA the inner region is being equipped with a small scintillator based TOF detector [24], readout by 24 commercial single pixel HPD's fabricated by DEP. The HPD's work in an axial magnetic field of 1.1 T.

- Ring Imaging Cherenkov (RICH) detectors
  The detection of Cherenkov photons in RICH counters requires photodetectors with a high sensitivity in the visible and UV part of the light spectrum combined with a spatial resolution in the mm range. Another prerequisite for the efficient reconstruction of Cherenkov patterns is a large active area coverage fraction, a feature which is not offered by currently available HPD's.

We discuss in the following the development of large area HPD's for the LHCb [25] experiment. After a short introduction to the experiment and its two RICH detectors, two parallel R&D programs will be described.

4.2. The LHCb experiment

The single arm spectrometer LHCb is designed for CP asymmetry and rare decay studies in the system of B-mesons. LHCb will profit from the high $b\bar{b}$ cross section and luminosity at the LHC collider. The outline of the recently approved LHCb spectrometer is shown in Fig. 7. It includes two RICH detectors for π/K separation in the momentum range 1-150 GeV/c. The Cherenkov light emitted from the various radiators (Aerogel, CF_4 gas, C_4F_{10} gas) is focused by means of spherical mirrors onto detection planes outside the acceptance of the LHCb spectrometer. In total a surface of 2.9 m^2 has to be equipped with photodetectors which have to provide a granularity of about 2.5×2.5 mm^2. Hexagonal close packing of round photodetectors with an active surface coverage of 80% results in a total number of electronic channels of about 340,000.

Comprehensive R&D programmes [26–28] have been launched to develop large area HPD's adequate for the LHCb requirements. In addition to the high active area fraction, fast LHC speed readout electronics is a key requirement of the photodetectors. As

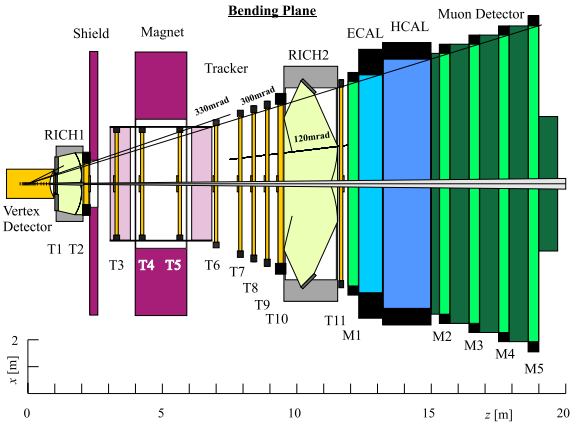

Figure 7. Outline of the LHCb spectrometer. The two RICH detectors are positioned behind the microvertex detector (RICH 1) and in front of the electromagnetic calorimeter (RICH 2).

a backup solution the Hamamatsu multi anode PMT R5900/64 is under investigation [29,30]. In this case an additional lens system as well as minor modifications of the tube design are necessary in order to reach a sufficiently high surface coverage.

4.3. The 5-inch pad HPD project

The HPD, as shown in Fig. 8, consists of a cylindrical vacuum glass envelope of 127 mm diameter with a spherical entrance window made of borosilicate glass. A visible light transmittive bialkali photocathode (K_2CsSb) is vacuum evaporated on the inside surface of the window. The photoelectrons are accelerated by a potential difference of the order of 20 kV onto a silicon sensor of 50 mm active diameter. Focusing ring electrodes produce a fountain-like electrostatic field geometry, which results in a linear demagnification of 2.7 over the full geometrically accepted diameter of 114 mm. The silicon sensor consisting of 16 sectors with in total 2048 pads (each $\approx$ 1 $\times$ 1 mm^2) is mounted on a 4-layer ceramic printed circuit board. Wire bonds feed the signals to 16 VA3 [31] analogue readout chips (128 channels: pre-amplifier, shaper, sample & hold and multiplexer). Signal/noise ratios in excess of 20 have been obtained with this relatively slow electronics (shap-

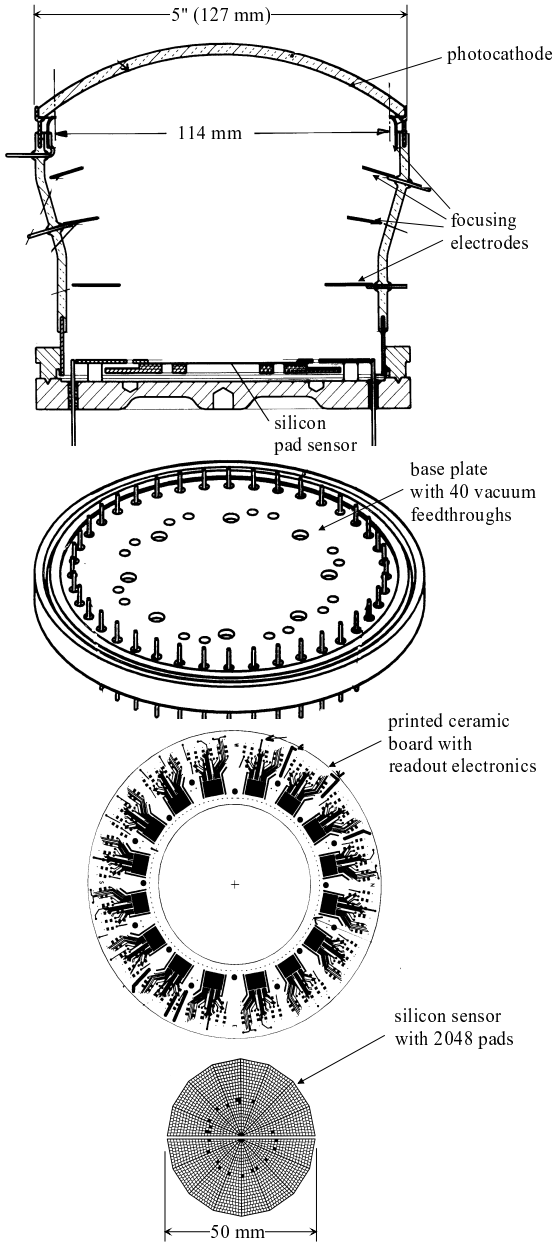

Figure 8. The upper figure shows a cross section of the 5-inch HPD. Below the the base plate, the ceramic printed board and the silicon sensor are depicted.

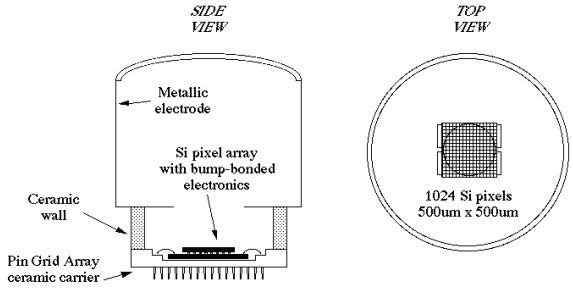

Figure 9. Schematic design of the 80 mm Pixel HPD.

ing time $\tau \approx 1.6\mu$s), where the tube could be operated at up to 30 kV. In the next phase of the project the VA3 will be replaced by the fast (25 ns peaking time) SCT128A analogue chip [32]. Details of the project, in particular a description of the manufacturing process (photocathode fabrication and subsequent encapsulation in an ultrahigh vacuum plant built at CERN), and its status are given in [33].

4.4. The 80 mm pixel HPD project

The 80 mm diameter HPD, which is schematically shown in Figure 9, employs the cross focusing technique. In its final version the image of the 72 mm active diameter photocathode is demagnified by a factor 4 onto a silicon sensor consisting of 1024 pixels of 500×500 μm^2 each. A binary readout chip is bump bonded to the pixel array. The tube is developed in collaboration with DEP. Two prototype tubes, one equipped with a phosphor screen / CCD readout and one with a DEP standard 61 pixel sensor will be available for tests in the nearest future. A half scale prototype, equipped with an Omega3 pixel chip (2048 pixels of 500×50 μm^2) each has already been tested in the LHCb RICH prototype set-up [34]. The Omega3 chip, originally designed for tracking application, is not optimised for single photoelectron detection at LHC speed: minimum threshold 3000 e^- (500 e^- RMS), 100 ns peaking time. As an intermediate step a test chip [35] with 25 ns peaking time and 1500 e^- threshold (25 e^- RMS) has been designed and successfully tested in collaboration with the ALICE tracking group.

5. Summary

Hybrid Photodiodes, although developed more than 30 years ago, have received attention by the high energy physics community only in the more recent past. The HPD's combine the sensitivity of photomultipliers with the spatial and energy resolution of silicon detectors, which leads to a superb photon counting capability. Further features of the HPD principle are the high intrinsic speed, the excellent linearity and the possibility to operate proximity focused devices in strong magnetic fields. HPD's appear as interesting candidates for numerous applications in calorimetry, fibre tracking, Cherenkov counting as well as for applications outside high energy physics . All commercially available devices, however, exhibit only low active surface coverage fractions which are inacceptable for Ring Imaging Cherenkov detection. To remove this obstacle, high granularity HPD's with optimised area coverage are currently under development for the LHCb experiment.

Acknowledgements

I would like to thank C. D'Ambrosio, T. Gys, J. Séguinot and T. Ypsilantis for numerous fruitful discussions. I am grateful to E. Beaver, A. Duane, R. Forty and E. Lorenz for providing me with material and valuable background information for this paper. The continuous support and encouragement by O. Ullaland and E. Nappi was highly appreciated.

REFERENCES

1. C. D'Ambrosio et al., *Nucl. Instr. Meth. A338 (1994)* 396
2. T. Tabarelli de Fatis, *Nucl. Instr. Meth. A385 (1997)* 366
3. G. Bondarenko et al., *Nucl.Phys.B 61B (1998)* 347
4. S. Vasile et al., to be published in *Proceedings of the IEEE Nuclear Science Symposium*, Toronto, November 1998.
5. S. Buontempo et al., *CERN-EP/98-36, to be published in Nucl. Instr. Meth. A* 347
6. D. Lincoln et al., *these proceedings.*
7. F. A. White and J. C. Sheffield, *Proc. IRE, Vol. 50, No. 6 (1962)*.

8. A. V. Brown, *IEEE Trans. on Electron Devices, Vol. 10, No. 1 (196)* 8
9. R. Kalibjian, *IEEE Trans. on Nuclear Science, Vol. 12, No. 4 (1965)* 367
10. G. Wolfgang et al., *IEEE Trans. on Nuclear Science, Vol. 13, (1966)* 46
11. R. Kalibjian, *IEEE Trans. on Nuclear Science, Vol. 13, (1966)* 54
12. E. A. Beaver and C. E. McIlwain, *Rev. Sci. Instruments, Vol. 42, No. 9 (1971)* 1321
13. R. Harms et al. *NASA CP-2244 (1982)* 55
14. R. DeSalvo, *Cornell University, preprint, CLNS87-92 (1987)*
15. R. DeSalvo, *Nucl. Instr. Meth. A315 (1992)* 375
16. T. Gys et al., *Nucl. Instr. Meth. A355 (1995)* 386
17. T. Gys et al., *Nucl. Instr. Meth. A387 (1997)* 131
18. M. Suyama et al., A Compact Hybrid Photodetector (HPD), *Hamamatsu Photonics K.K., Internal note.*
19. S.M. Bradbury et al., *Nucl. Instr. Meth. A387 (1997)* 45
20. E. Lorenz et al., *these proceedings.*
21. C. D'Ambrosio et al., *these proceedings.*
22. H. Arnaudon et al., *Nucl. Instr. Meth. A342 (1994)* 558
23. CMS Technical Design Report 2, HCAL *CERN LHCC 97-31*
24. V. Filippini et al., *these proceedings.*
25. LHCb Technical Proposal. *CERN/LHCC 98-4, LHCC/P4*
26. E. Chesi et al., *LHC-B/96-010*
27. E. Chesi et al., *Nucl. Instr. Meth. A387 (1997)* 122
28. M. Campbell et al., *LHCb 98-035*
29. A. Duane et al., *LHCb 98-39*
30. R. Forty, *LHCb 98-38*
31. P. Weilhammer et al., *Nucl. Instr. Meth. A383 (1996)* 89
32. S. Anghinolfi et al., *IEEE Trans. Nucl. Sci. 44 (1997)* 298
33. A. Braem et al., *these proceedings.*
34. M. Alemi et al., *these proceedings.*
35. M. Campbell et al., to be published in *Proceedings of the IEEE Nuclear Science Symposium*, Toronto, November 1998.